Control Engineering Practice 21 (2013) 1259–1265

Contents lists available at SciVerse ScienceDirect

Control Engineering Practice

journal homepage: www.elsevier.com/locate/conengprac

Second-order sliding mode observer for multiple kinetic rates estimation in bioprocesses

Sebastián Nuñez [a,b,*], Hernán De Battista [a,b], Fabricio Garelli [a,b], Alejandro Vignoni [c], Jesús Picó [c]

[a] CONICET, Argentina
[b] LEICI, Facultad de Ingeniería, Universidad Nacional de La Plata (UNLP), Calle 48 esq. 116s/n, La Plata, Argentina
[c] Institut d'Automàtica i Informàtica Industrial, Universitat Politècnica de València, Camí de Vera s/n, Valencia, Spain

ARTICLE INFO

Article history:
Received 7 December 2012
Accepted 9 March 2013
Available online 12 May 2013

Keywords:
Bioprocess control
High-order sliding modes
Sliding observer
Kinetic rates
Software sensor

ABSTRACT

Specific kinetic rates are key variables regarding metabolic activity in bioprocesses. They are non-linear functions of concentrations and operating conditions and therefore of difficult access for process control. In this paper, a multiple kinetic rates observer based on second-order sliding mode ideas is proposed. The main difference with other proposals is that smooth estimates are achieved in finite-time without adding additional dynamics. The resulting estimator is robust against uncertainty in the model of the estimated variables. Experimental results from continuous fermentation of *S. cerevisiae* are presented, where microbial specific growth rate and net ethanol production rate are estimated.

1. Introduction

Nowadays, biotechnological processes are applied in a wide range of industries for the production of enzymes, recombinant proteins, and high-value metabolic products. An important control problem of these processes is to achieve a desired metabolic condition (Jobé et al., 2003). The specific reaction rates contain information that is closely related to microbial activity. The knowledge of these signals have at least two relevant applications. First, reaction rates can be used in closed-loop control for improving process productivity. For instance, certain industrial problems have been related to the problem of regulating the specific growth rate (μ) of microorganism (Ren & Yuan, 2005; Soons, Voogt, van Straten, & van Boxtel, 2006). Second, the on-line availability of such information during the cultivation stage enhances bioprocess monitoring, which is essential for quality control, process reproducibility and early problem detection (Vojinovi, Cabral, & Fonseca, 2006).

Regretfully, specific reaction rates are in general not accessible since they are unmeasurable and uncertain non-linear functions of states (concentrations) and operating conditions (temperature, pH, pressure, etc). In this context, the use of observers (*software sensors*) to obtain an on-line estimation of specific rates avoids the problem of model identification while adds information for closed-loop control schemes and culture studies (Farza, Busawon, & Hammouri, 1998).

A survey of relevant methods applied to state estimation in bioprocesses can be found in Venkateswarlu (2004). Particularly, several model-based observers have been proposed for the reaction rate estimation problem. They include adaptive estimator for microbial growth rate in Bastin and Dochain (1986), extended Kalman filter in Shimizu, Takamatsu, Shioya, and Suga (1989), asymptotic observers for parameter estimation in Bastin and Dochain (1990), high gain observers of specific rates in Farza et al. (1998), Gauthier, Hammouri, and Othman (1992), and Martinez-Guerra, Garrido, and Osorio-Miron (2001), and sliding mode based observers in Picó, De Battista, and Garelli (2009), Rahman, Spurgeon, and Yan (2010), and De Battista, Picó, Garelli, and Vignoni (2011). Other approach, which does not rely on process model but requires training data sets, is based on artificial neural networks (Karakuzu, Türker, & Öztürk, 2006).

In the sliding mode observers (SMO), the idea is to enforce a sliding regime on the subspace for which the state estimation error is zero by means of a discontinuous action. Then, the observer output copies the measured state despite disturbances and allows the reconstruction of the signal of interest (De Battista, Picó, Garelli, & Navarro, 2012; Edwards & Spurgeon, 1998). In the problem of kinetic rates estimation, the unknown signals appear

* Corresponding author at: LEICI, C.C. 91 (1900), La Plata, Argentina. Tel./fax: +54 221 425 9306.
E-mail addresses: sebastian.nuniez@ing.unlp.edu.ar (S. Nuñez), deba@ing.unlp.edu.ar (H. De Battista), fabricio@ing.unlp.edu.ar (F. Garelli), alvig2@upv.es (A. Vignoni), jpico@ai2.upv.es (J. Picó).

0967-0661/$ - see front matter © 2013 Elsevier Ltd. All rights reserved.
http://dx.doi.org/10.1016/j.conengprac.2013.03.003

in the time-derivative of the states. First-order sliding mode observers were developed in Picó et al. (2009) to deal with specific growth rate and substrate estimation from on-line biomass measurement. Although the exact estimation of μ was a high-frequency discontinuous signal, it was useful for constructing the substrate observer. The resulting estimates were robust under typical model uncertainties while exhibiting first order dynamics. In Rahman et al. (2010), substrate measurements were used to estimate the substrate consumption rate. The observer error dynamics is exponentially stable whereas model uncertainties and disturbances are rejected. Thereafter, in De Battista et al. (2011) a second-order sliding mode observer of μ was presented. More precisely, the proposal is a modified version of the "super twisting" algorithm, a high-order sliding mode algorithm presented in Levant (1998). In this case, the observer provides smooth estimation that exhibits finite-time convergence and is robust to typical process model uncertainties.

This work is intended to generalise preliminary results in De Battista et al. (2011). The multiple rates estimation problem requires to deal with an additional time-varying function. Therefore, further modifications are required in both the observer's structure as in the proposition of stability conditions. From bioprocess control viewpoint, the goal is to add information about the microorganism activity so as to increase on-line signals for closed-loop control and bioprocess monitoring. Therefore, the observer proposed here is applied to estimate p specific kinetic rates of production or consumption based on p related on-line measurements of process variables. The main difference with other continuous time proposals is that the estimates are achieved in finite-time and from then on, no additional dynamics is added. Besides, differing from first-order SM proposals the resulting estimations are smooth. Consequently, no additional smoothing elements would be required in closed-loop configurations. Further, robustness is expected since no model of each kinetic rate is assumed.

The rest of the paper is organised as follows. In Section 2 the problem to be solved and a typical state-space model for a bioprocess in a stirred-tank are presented. Then, in Section 3, the proposed observer is formulated. Section 4 presents results in which microbial specific growth rate and net ethanol production rate in continuous fermentation of *Saccharomyces cerevisiae* are estimated from experimental data. Finally, in Section 5, concluding remarks are given.

2. Bioprocess model and problem statement

A biotechnological process taking place in a stirred tank can be described by the following state-space model (Bastin & Dochain, 1990):

$$\frac{d\boldsymbol{\xi}}{dt} = \boldsymbol{K}\boldsymbol{r}(\boldsymbol{\xi},t) - D(t)\boldsymbol{\xi}(t) + \boldsymbol{F}(t) - \boldsymbol{Q}(\boldsymbol{\xi}), \tag{1}$$

where $\boldsymbol{\xi}(t)\in\mathbb{R}^n_+$ is the state vector, $\boldsymbol{K}$ an $(n\times m)$ pseudo-stoichiometric coefficients matrix, $\boldsymbol{r}(\cdot)\in\mathbb{R}^m$ the reaction rates vector, $D(t)\in\mathbb{R}_+$ the dilution rate, $\boldsymbol{F}(t)\in\mathbb{R}^n_+$ the input flow rate vector and $\boldsymbol{Q}(\boldsymbol{\xi})\in\mathbb{R}^n_+$ the gaseous outflow rate vector.

Eq. (1) describes the dynamics of the (bio)chemical species in the culture, which evolves according to m reaction rates $\boldsymbol{r}(\boldsymbol{\xi},t)$. Since the reactions can take place only in the presence of certain necessary reactants, $r_i(\cdot)$ is zero whenever the concentration of one of the required reactants is zero. Then, the reactions can be factorised as $r_i(\boldsymbol{\xi},t)=\alpha_i(\boldsymbol{\xi},t)\prod_{j\in\mathcal{J}_i}\xi_j$ where $\alpha_i(\cdot)$ is generally a non-linear function and $\mathcal{J}_i$ denotes the set of required reactants (Bastin & Dochain, 1990). In matrix form, this results in

$$\boldsymbol{r}(\boldsymbol{\xi},t) = \boldsymbol{G}(\boldsymbol{\xi},t)\boldsymbol{\alpha}(\boldsymbol{\xi},t), \tag{2}$$

where $\boldsymbol{G}(\boldsymbol{\xi},t)$ is an $(m\times m)$ state-dependent diagonal matrix.

The $\alpha_i(\cdot)$ defined in (2) are called the *specific* reaction rates per unit of *each* reactant (other definitions such as per unit of biomass are usually used, see Perrier, Feyo de Azevedo, Ferreira, & Dochain, 2000). These non-linear time-varying functions provide important knowledge about the bioprocess (e.g. microbial specific growth rate, oxygen specific uptake rate, specific production rate of metabolites) but its modelling and parameter identification can be extremely difficult. In order to add information about the process (possibly for on-line process control), a software sensor of specific reaction rates will be developed.

Particularly, the goal is to derive a robust observer of a subset of p specific reaction rates, namely $\boldsymbol{\alpha}_p(t)=[\alpha_1(t),\ldots,\alpha_p(t)]^T$. To this end, let us consider that p available measurements of $\boldsymbol{\xi}(t)$ are rearranged in a vector $\boldsymbol{z}$, i.e. $\boldsymbol{z}(t)=[\xi_1(t),\ldots,\xi_p(t)]^T$. Let $\boldsymbol{K}_p$ and $\boldsymbol{G}_p(\cdot)$ be the corresponding $(p\times p)$ submatrices of $\boldsymbol{K}$ and $\boldsymbol{G}(\cdot)$, respectively whereas $\boldsymbol{F}_p$ and $\boldsymbol{Q}_p$ are the corresponding $(p\times 1)$ vectors arranged from $\boldsymbol{F}$ and $\boldsymbol{Q}$. Assume the following:

Assumption 1. The state variables are positive and bounded.

Assumption 2. $\boldsymbol{G}_p$, $\boldsymbol{F}_p$ and $\boldsymbol{Q}_p$ are available.

Assumption 3. A bound for each α_i time derivative $\overline{\rho}_i>0$ is known.

Assumption 4. The matrix $\boldsymbol{K}_p$ is invertible.

Assumption 5. Diagonal matrices $\boldsymbol{G}_1$, $\boldsymbol{G}_2$ such that $\boldsymbol{0}<\boldsymbol{G}_1\leq \boldsymbol{G}_p(\cdot)\leq\boldsymbol{G}_2$ holds are known.

Note that Assumption 1 holds for the bioprocess variables (e.g. component concentrations and volume). Assumption 2 is a common assumption in the literature regarding the availability of certain on-line measurements (e.g Perrier et al., 2000). Assumption 3 states that a bound of each kinetic dynamics is available, which can be determined from practice knowledge of the bioprocess. Assumption 4 ensures that p reaction rates can be estimated from the p measured variables. Otherwise, the measured vector would not provide enough information about the reactions. From the discussion of Eq. (2), the elements of $\boldsymbol{G}_p$ are products of state variables which all remain positive and bounded. In the event that one required reactant vanishes, then at least one reaction no longer takes place. In that case, the estimation of the reaction rate has no sense and consequently the estimation problem should be reconsidered. The diagonal elements of $\boldsymbol{G}_1$ and $\boldsymbol{G}_2$ in Assumption 5 should be selected by the user based on his own knowledge about the particular process being monitored.

Now, from the model (1) and the previous discussion, the following system is considered

$$\frac{d\boldsymbol{z}}{dt} = \boldsymbol{K}_p\boldsymbol{G}_p(\cdot)\boldsymbol{\alpha}_p(\boldsymbol{\xi},t) - D\boldsymbol{z} + \boldsymbol{F}_p - \boldsymbol{Q}_p, \tag{3}$$

$$\frac{d\boldsymbol{\alpha}_p}{dt} = \boldsymbol{R}\boldsymbol{\rho}(t), \tag{4}$$

in which $\boldsymbol{\alpha}_p(t)$ is the vector of specific kinetic rates to be estimated and $\boldsymbol{R}=diag\{\overline{\rho}_i\}$ arranges the bounds of the time derivatives. Note that $\boldsymbol{\rho}(t)$ is a vector of p unknown continuous functions where $\|\boldsymbol{\rho}(t)\|_\infty\leq 1$ holds.

3. A second-order observer of specific kinetic rates

3.1. Definitions

In this section the following notation is used:

$$\boldsymbol{G}_o = (\boldsymbol{G}_1 + \boldsymbol{G}_2)/2, \tag{5a}$$

$$\Delta\boldsymbol{G} = (\boldsymbol{G}_2 - \boldsymbol{G}_1)/2, \tag{5b}$$

$$\delta = \|\boldsymbol{G}_o^{-1}\Delta\boldsymbol{G}\|_\infty, \tag{5c}$$

$$\check{\boldsymbol{G}}_p(\cdot) = \boldsymbol{G}_o^{-1}\boldsymbol{G}_p(\cdot), \tag{5d}$$

where $\|\cdot\|_\infty$ stands here for the induced ∞-norm of the matrix.

Remark 1. Recalling definition and assumptions for $\boldsymbol{K}_p$, $\boldsymbol{G}_o$ and $\boldsymbol{R}$, it is straightforward to see that $\boldsymbol{K}_p\boldsymbol{G}_o\boldsymbol{R}$ is nonsingular.

Let define an auxiliary vector $\boldsymbol{\sigma}$ as

$$\boldsymbol{\sigma} = (\boldsymbol{K}_p\boldsymbol{G}_o\boldsymbol{R})^{-1}(\boldsymbol{z} - \hat{\boldsymbol{z}}), \tag{6}$$

where $\hat{\boldsymbol{z}}$ is an estimation of $\boldsymbol{z}$.

Finally, let SIGN$(\cdot)$: $\mathbb{R}^p \to \mathbb{R}^p$, ABS$(\cdot)$: $\mathbb{R}^p \to \mathbb{R}^{p\times p}$, defined as

$$\text{SIGN}(\boldsymbol{\sigma}) = col(sign(\sigma_i)), \tag{7}$$

$$\text{ABS}(\boldsymbol{\sigma}) = diag\{|\sigma_i|\}. \tag{8}$$

From Eq. (6), it follows that if there exists $T^* > 0$ such that $\boldsymbol{\sigma} \equiv \boldsymbol{0}$ holds for all $t > T^*$, i.e. if the system can be steered to evolve over the sliding surface defined by $\boldsymbol{\sigma}(\boldsymbol{z}) = \boldsymbol{0}$ in finite-time, then $\hat{\boldsymbol{z}} \equiv \boldsymbol{z}$ is achieved.

Since the previous comment is the core idea to estimate the reaction rates, the objective now is the design of a dynamic system which enforces Eq. (6) to vanish in finite-time.

3.2. Main result

Proposition 1. *The system defined by*

$$\frac{d\hat{\boldsymbol{z}}}{dt} = \boldsymbol{K}_p(\boldsymbol{G}_p(\cdot)\boldsymbol{R}\boldsymbol{u}_1 + 2k_2\boldsymbol{G}_o\boldsymbol{R}\boldsymbol{u}_2) - D\boldsymbol{z} + \boldsymbol{F}_p - \boldsymbol{Q}_p, \tag{9a}$$

$$\frac{d\boldsymbol{u}_1}{dt} = k_1\text{SIGN}(\boldsymbol{\sigma}), \tag{9b}$$

$$\boldsymbol{u}_2 = (\text{ABS}(\boldsymbol{\sigma}))^{1/2}\text{SIGN}(\boldsymbol{\sigma}), \tag{9c}$$

$$\hat{\boldsymbol{\alpha}} = \boldsymbol{R}\boldsymbol{u}_1, \tag{9d}$$

is a second-order sliding mode observer for (3)–(4). There exists suitable design constants $k_1 > 1$ and $k_2 > 0$ for which finite-time convergence of specific reaction rates, i.e. $\hat{\boldsymbol{\alpha}}(t) \equiv \boldsymbol{\alpha}_p(t)$ $\forall t > T^*$ for some finite $T^* > 0$, is achieved.

In order to prove Proposition 1, given $\tilde{\boldsymbol{\alpha}} = \boldsymbol{\alpha}_p - \hat{\boldsymbol{\alpha}}$, the error coordinates dynamics $(\boldsymbol{\sigma}, \tilde{\boldsymbol{\alpha}})$ is

$$\frac{d\boldsymbol{\sigma}}{dt} = \boldsymbol{R}^{-1}(\check{\boldsymbol{G}}_p(\cdot)\tilde{\boldsymbol{\alpha}} - 2k_2\boldsymbol{R}\boldsymbol{u}_2), \tag{10}$$

$$\frac{d\tilde{\boldsymbol{\alpha}}}{dt} = \boldsymbol{R}(\boldsymbol{\rho}(t) - k_1\text{SIGN}(\boldsymbol{\sigma})). \tag{11}$$

Applying the change of coordinates $(\boldsymbol{x}_1, \boldsymbol{x}_2) = (\boldsymbol{R}\boldsymbol{u}_2, \tilde{\boldsymbol{\alpha}})$ to system (9), yields

$$\frac{d\boldsymbol{x}_1}{dt} = \boldsymbol{R}(\text{ABS}(\boldsymbol{x}_1))^{-1}\left(-k_2\boldsymbol{x}_1 + \frac{\check{\boldsymbol{G}}_p(\cdot)}{2}\boldsymbol{x}_2\right), \tag{12}$$

$$\frac{d\boldsymbol{x}_2}{dt} = \boldsymbol{R}(\text{ABS}(\boldsymbol{x}_1))^{-1}(\text{ABS}(\boldsymbol{x}_1)\boldsymbol{\rho}(t) - k_1\boldsymbol{x}_1), \tag{13}$$

where the identities

$$\text{SIGN}(\boldsymbol{x}_1) = \text{SIGN}(\boldsymbol{\sigma}),$$

$$\text{ABS}(\boldsymbol{x}_1) = \boldsymbol{R}(\text{ABS}(\boldsymbol{\sigma}))^{1/2},$$

were used (see Eq. (9c)).

Recalling definitions (5a)–(5d) it is seen that

$$\boldsymbol{G}_p(\cdot) \in \{\boldsymbol{G}_o + \Delta\boldsymbol{G}\boldsymbol{U}_p\}, \tag{14a}$$

$$\check{\boldsymbol{G}}_p(\cdot) \in \{\boldsymbol{I}_p + \boldsymbol{G}_o^{-1}\Delta\boldsymbol{G}\boldsymbol{U}_p\}, \tag{14b}$$

where $\boldsymbol{I}_p$ denotes the $(p \times p)$ identity matrix and $\boldsymbol{U}_p$ is a $(p \times p)$ diagonal matrix such that $\|\boldsymbol{U}_p\|_\infty \le 1$.

Therefore, using (14) the following differential inclusion holds:

$$\frac{d\boldsymbol{x}}{dt} \in \begin{pmatrix} \boldsymbol{R}[\text{ABS}(\boldsymbol{x}_1)]^{-1} & \boldsymbol{0} \\ \boldsymbol{0} & \boldsymbol{R}[\text{ABS}(\boldsymbol{x}_1)]^{-1} \end{pmatrix} \begin{pmatrix} -k_2\boldsymbol{I}_p & \frac{1}{2}(\boldsymbol{I}_p + \delta\boldsymbol{U}_p) \\ -(k_1\boldsymbol{I}_p - \boldsymbol{U}_p) & \boldsymbol{0} \end{pmatrix} \boldsymbol{x}. \tag{15}$$

Now, given the ith kinetic rate arrange a vector $\boldsymbol{\zeta}_i$ with the ith components of $\boldsymbol{x}_1$ and $\boldsymbol{x}_2$ (i.e. $\boldsymbol{\zeta}_i = [x_{1i}\ x_{2i}]^T$). The corresponding differential inclusion is

$$\frac{d\boldsymbol{\zeta}_i}{dt} = \frac{\overline{\rho}_i}{|x_{1i}|}\boldsymbol{A}(t)\boldsymbol{\zeta}_i \in \frac{\overline{\rho}_i}{|x_{1i}|}\begin{pmatrix} -k_2 & \frac{1}{2}(1 + \delta U_i) \\ -(k_1 - U_i) & 0 \end{pmatrix}\boldsymbol{\zeta}_i, \tag{16}$$

where U_i is the (i,i) entry of $\boldsymbol{U}_p$.

It will be shown that each of these coordinates converges in finite time to the origin independently of the others. For this purpose, the candidate Lyapunov function $V(\boldsymbol{\zeta}_i) = \sum_i \boldsymbol{\zeta}_i^T\boldsymbol{P}\boldsymbol{\zeta}_i$ (Moreno & Osorio, 2008) is considered. The time derivative of $V(t)$ results in

$$\dot{V}(t) = \sum_i \frac{\overline{\rho}_i}{|x_{1i}|}\boldsymbol{\zeta}_i^T\left(\boldsymbol{A}^T(t)\boldsymbol{P} + \boldsymbol{P}\boldsymbol{A}(t)\right)\boldsymbol{\zeta}_i, \tag{17}$$

with $\boldsymbol{A}(t)$ given in (16). The goal is to determine $\boldsymbol{P} > 0$ such that $\dot{V}(t) < 0$ along any non-zero solution of Eq. (16). To this end, consider the following proposition.

Proposition 2. *Consider the polytopic linear differential inclusion*

$$\dot{\boldsymbol{\zeta}} = \boldsymbol{A}(t)\boldsymbol{\zeta}, \quad \boldsymbol{A}(t) \in \mathcal{A} \tag{18}$$

with

$$\mathcal{A} = co\bigcup_i \boldsymbol{A}_i, \quad i = 1, \ldots, 4$$

$$\boldsymbol{A}_i = \begin{bmatrix} -k_2 & \frac{1}{2}(1 + \delta v_i) \\ -(k_1 - u_i) & 0 \end{bmatrix},$$

$$u = \{-1, -1, 1, 1\}, \quad v = \{-1, 1, -1, 1\}. \tag{19}$$

Then, for every $k_1 > 1$ and $0 < \delta < 1$ there exists suitable values of k_2 such that (18) is quadratically stable for all $\boldsymbol{A}(t) \in \mathcal{A}$.

Stability of system (18) was proved in De Battista et al. (2011) for the case $\delta = 0$ with the Lyapunov function $V(\boldsymbol{\zeta}) = \boldsymbol{\zeta}^T\boldsymbol{P}\boldsymbol{\zeta}$. This proposition is an extension of the one proposed in De Battista et al. (2011) to deal with $\delta > 0$. The main difference consists in the requirement of a grid covering the space (k_1, δ) instead of k_1 in order to include all the possible systems described by Eq. (18).

A polytopic linear differential inclusion is said quadratically stable if there exists $V(\boldsymbol{\zeta}) = \boldsymbol{\zeta}^T\boldsymbol{P}\boldsymbol{\zeta}$, $\boldsymbol{P} > 0$ that decreases along every non-zero trajectory of system (18).

Since $\dot{V}(\boldsymbol{\zeta}) = \boldsymbol{\zeta}^T(\boldsymbol{A}^T(t)\boldsymbol{P} + \boldsymbol{P}\boldsymbol{A}(t))\boldsymbol{\zeta}$, a necessary and sufficient condition for quadratic stability is

$$\boldsymbol{P} > 0,$$

$$\boldsymbol{A}^T(t)\boldsymbol{P} + \boldsymbol{P}\boldsymbol{A}(t) < 0 \quad \forall \boldsymbol{A}(t) \in \mathcal{A}. \tag{20}$$

This is equivalent to determine the existence of a common Lyapunov matrix $\boldsymbol{P}$ for all the vertices of the polytope $\mathcal{A}$, i.e. that

verifies the following constraints:

$$\mathcal{F}=\left\{\begin{array}{l}\boldsymbol{P}>0\\ \boldsymbol{Q}_i\triangleq-(\boldsymbol{A}_i^T\boldsymbol{P}+\boldsymbol{P}\boldsymbol{A}_i)>0\end{array}\right\}. \tag{21}$$

for $i=1\ldots4$.

Now rewriting A_i in a convenient way,

$$\boldsymbol{A}_i=k_2\boldsymbol{A}_0+\boldsymbol{A}_i^*, \tag{22}$$

where

$$\boldsymbol{A}_0=\begin{bmatrix}-1 & 0\\ 0 & 0\end{bmatrix},$$
$$\boldsymbol{A}_1^*=\begin{bmatrix}0 & \frac{1}{2}(1+\delta)\\ -(k_1-1) & 0\end{bmatrix},$$
$$\boldsymbol{A}_2^*=\begin{bmatrix}0 & \frac{1}{2}(1+\delta)\\ -(k_1+1) & 0\end{bmatrix},$$
$$\boldsymbol{A}_3^*=\begin{bmatrix}0 & \frac{1}{2}(1-\delta)\\ -(k_1-1) & 0\end{bmatrix},$$
$$\boldsymbol{A}_4^*=\begin{bmatrix}0 & \frac{1}{2}(1-\delta)\\ -(k_1+1) & 0\end{bmatrix}. \tag{23}$$

The existence of a common Lyapunov $\boldsymbol{P}$ for any $k_1>1$ and $0<\delta<1$ can be determined by checking the feasibility of the following generalised eigenvalue problem (GEVP) in $\boldsymbol{P}$ and k_2 (Boyd, El Ghaoui, Feron, & Balakrishnan, 1994):

$$\begin{array}{l}\min\quad k_2\\ \text{s.t.}\quad k_2>0,\quad \boldsymbol{P}>0,\quad \mathcal{F}^*,\end{array} \tag{24}$$

with

$$\mathcal{F}^*=\{(\boldsymbol{A}_i^{*T}\boldsymbol{P}+\boldsymbol{P}\boldsymbol{A}_i^*)+k_2(\boldsymbol{A}_0^T\boldsymbol{P}+\boldsymbol{P}\boldsymbol{A}_0)<0\}, \tag{25}$$

for $i=1\ldots4$.

A GEVP is a quasi-convex optimisation problem. In this case, it can be solved using a bisection algorithm on k_2 and determining the feasibility of the remaining linear matrix inequality (LMI). A grid covering the desired values of k_1 for some desired value δ was made, and the corresponding LMIs were solved with YALMIP (Löfberg, 2012). Fig. 1 shows the set of values of k_1 and k_2 for which the LMI problem is feasible, for different values of the parameter δ. For all points within the resulting sets of parameters, Proposition 2 holds.

Now, values of k_1 and k_2 for Proposition 1 follow from the application of Proposition 2. That is, given $k_1>1$ and certain δ, the value of k_2 is selected such that Eq. (18) is quadratically stable. Recall that δ stands for the maximum element of $\|\boldsymbol{G}_o^{-1}\Delta\boldsymbol{G}\|$ thus this value is suitable to get $\dot{V}(t)<0$ for all the reaction rates.

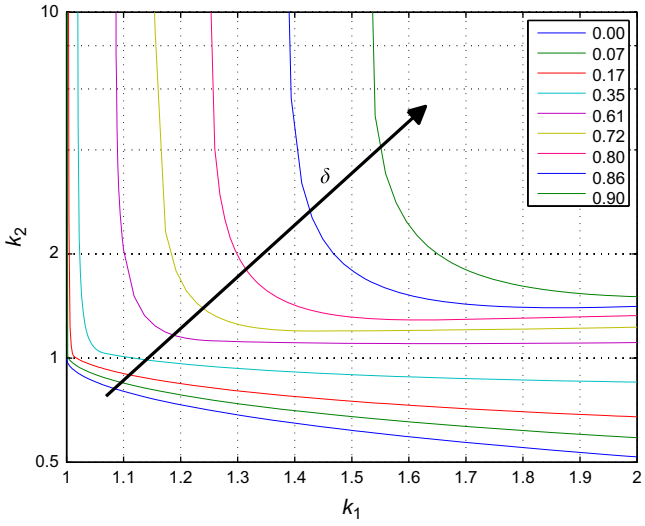

Fig. 1. Values of k_1 and k_2 for which system (18) is quadratically stable.

Finally, for suitable k_1 and k_2 the system reaches a neighbourhood of the sliding surface and thus the sliding-mode regime is established. From then on, the so-called *invariance condition* ($\boldsymbol{\sigma}\equiv\boldsymbol{0}$) holds (Utkin, Guldner, & Shi, 1999). Consequently, for certain T^*, $\hat{\boldsymbol{z}}(t)\equiv\boldsymbol{z}(t)\quad\forall t>T^*$. By equating expressions (3) and (9a), $\hat{\boldsymbol{\alpha}}(t)=\boldsymbol{\alpha}_p(\boldsymbol{\xi},t)$ is obtained. Note in Eq. (9c) that when the system is restricted to the sliding surface $\boldsymbol{\sigma}=\boldsymbol{0}$ the matrix ABS($\boldsymbol{\sigma}$) is the zero matrix, and thus $\boldsymbol{u}_2=\boldsymbol{0}$.

4. Experimental results

In this section, the sliding mode observer developed in Section 3 is evaluated experimentally. The application consists in estimating the specific production rate of ethanol (q_e) and the specific growth rate (μ) of the strain *S. cerevisiae* (T73) in a continuous-mode fermentation. To this end, on-line measurements of biomass (x) and ethanol (e) concentrations were collected. Biomass measurements were taken with a sensor based on measurement of the optical density (Navarro, Pico, Bruno, Pico-Marco, & Valles, 2001). Samples taken every 12 s are filtered over a time-window of 120 s. Ethanol concentration was monitored using a Raven Biotech's stand-alone methanol sensor with sample time of 120 s. The volume was 3L and the total fermentation time was 93 h. During the first 23 h batch cultivation was carried out. After that, the dilution rate profile shown with dash-dotted line in Fig. 3 was applied. A set-point step in D from 0.18 to 0.22h^{-1} is produced at $t\approx50$ h.

The proposal is assessed for two possible scenarios. First, the SMO is tested in the conditions described above and second, the observer is evaluated for two typical sensor failures which were digitally generated. In the latter case, the results are compared with a high gain observer. Particularly, the continuous time estimator described by

$$\frac{d}{dt}\begin{pmatrix}\hat{x}\\ \hat{e}\end{pmatrix}=\begin{pmatrix}\hat{x} & 0\\ 0 & \hat{x}\end{pmatrix}\begin{pmatrix}\hat{\mu}\\ \hat{q}_e\end{pmatrix}-\frac{F_{in}}{v}\begin{pmatrix}\hat{x}\\ \hat{e}\end{pmatrix}-2\theta_1\begin{pmatrix}\hat{x}-x\\ \hat{e}-e\end{pmatrix}, \tag{26a}$$

$$\frac{d}{dt}\begin{pmatrix}\hat{\mu}\\ \hat{q}_e\end{pmatrix}=\frac{-\theta_1^2}{\hat{x}}\begin{pmatrix}\hat{x}-x\\ \hat{e}-e\end{pmatrix}, \tag{26b}$$

which is presented in Farza et al. (1998) was implemented.

The main difference of this class of observers with the SMO is that in the former there is an addition of dynamics. This fact is important regarding closed loop applications. For instance, if Eq. (26) is applied for feedback, $2p$ integrators are added to closed loop dynamics. Consequently, closed loop stability must be analysed when the feedback signals are taken from the high gain observer. The same comment holds for other algorithms such as asymptotic observers. On the other hand, the SM approach provides convergence in finite-time to the target variables and from then on no additional dynamics is added. This fact simplifies the control system design.

The mass-balance equations for the process are

$$\frac{dx}{dt}=\mu x-Dx \tag{27a}$$

$$\frac{ds}{dt}=q_s x+D(s_r-s), \tag{27b}$$

$$\frac{de}{dt}=q_e x-De, \tag{27c}$$

where $D=F_{in}/v$ is the dilution rate, s the substrate concentration,

s_r the input substrate concentration and ν the (constant) working volume.

Since x and e are the measured state variables, the corresponding subsystem is of dimension $p=2$. Note in (27) that μ and q_e are the specific kinetic rates per unit of biomass. The corresponding subsystem in the form of Eq. (3) is

$$\frac{d\boldsymbol{z}}{dt}=\begin{pmatrix}1 & 0\\ 0 & 1\end{pmatrix}\begin{pmatrix}x & 0\\ 0 & x\end{pmatrix}\begin{pmatrix}\mu\\ q_e\end{pmatrix}-D\boldsymbol{z}, \tag{28}$$

where $\boldsymbol{z}=[x\ e]^T$, $\boldsymbol{\alpha}_p=[\mu\ q_e]^T$ and $\boldsymbol{F}_p=\boldsymbol{Q}_p=\boldsymbol{0}$. In this factorisation $\boldsymbol{K}_p=\boldsymbol{I}_2$ and $\boldsymbol{G}_p=x\boldsymbol{I}_2$.

Therefore, matrices $\boldsymbol{G}_1$ and $\boldsymbol{G}_2$ (see Eqs. (5)) are determined bounding for above ($\overline{x}$) and below ($\underline{x}$) the expected biomass excursion. The values $\underline{x}=2\ \mathrm{g\ L^{-1}}$ and $\overline{x}=18\ \mathrm{g\ L^{-1}}$ were selected, which resulted in conservative enough bounds. Accordingly, the matrices $\boldsymbol{G}_1$ and $\boldsymbol{G}_2$ are

$$\boldsymbol{G}_1=2\boldsymbol{I}_2,$$

$$\boldsymbol{G}_2=18\boldsymbol{I}_2,$$

and therefore $\boldsymbol{G}_o=10\boldsymbol{I}_2$, $\Delta\boldsymbol{G}=8\boldsymbol{I}_2$ and $\delta=0.80$.

The bounds $\overline{\rho}_i$ were selected as 0.1 and 0.25, and therefore $\boldsymbol{R}=diag\{0.1\ 0.25\}$. These bounds can in practice be adjusted according to the previous experience about the bioprocess and from model simulations (De Battista et al., 2012; Perrier et al., 2000).

The resulting values of k_2 for several values of k_1 were obtained by solving the problem (24)–(25). These results are depicted in Fig. 1. It is seen for any δ that the lower is k_1, the greater is the minimum k_2. In order to get a feasible minimisation problem for $\delta=0.8$ with a small k_2, $k_1=1.35$ was selected. From problem (24)–(25), the minimum k_2 is 1.5715 and then $k_2=1.75$ was selected. Other possibility for the designing of the gains includes the adaptive-gain approach, see for instance Shtessel, Moreno, Plestan, Fridman, and Poznyak (2010) and Evangelista, Puleston, Valenciaga, and Fridman (2013).

4.1. Results

The SMO was initialised with the first samples, i.e. $\hat{\boldsymbol{z}}(t_0)=(x(t_0),e(t_0))$ and $(\hat{\mu}(t_0),\hat{q}_e(t_0))=(0,0)$. Fig. 2 shows biomass and ethanol time profiles and their corresponding variables $\hat{z}_1$ and $\hat{z}_2$ almost overlapped, respectively.

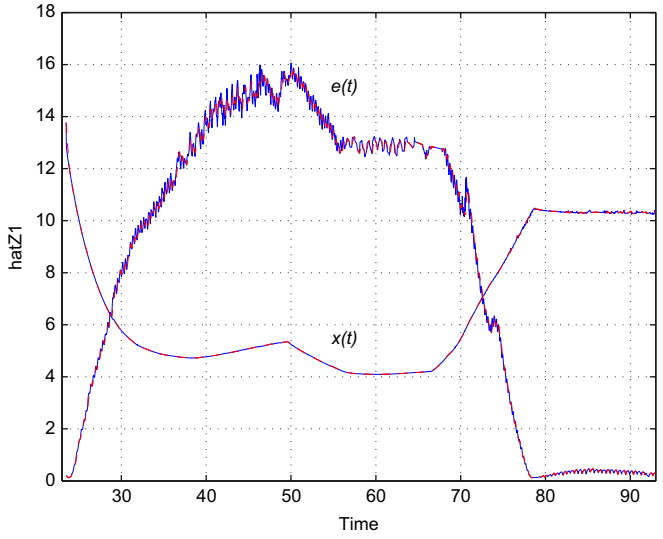

Fig. 2. Time profile of $x(t)$ (blue-solid), $\hat{x}(t)$ (red-dash) and $e(t)$ (blue-solid), $\hat{e}(t)$ (red-dash) in the continuous fermentation (27). (For interpretation of the references to color in this figure caption, the reader is referred to the web version of this article.)

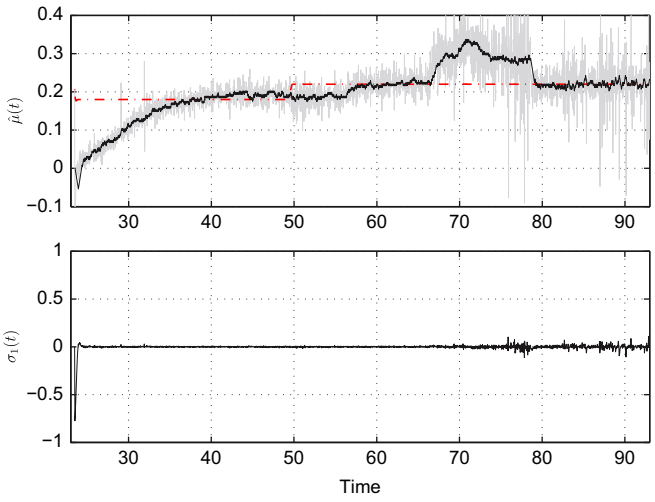

Fig. 3. Estimated specific growth rate $\hat{\mu}(t)$ with SMO (black) and Eq. (29) (grey), dilution rate (dash-dotted) (above); switching coordinate σ_1 (below).

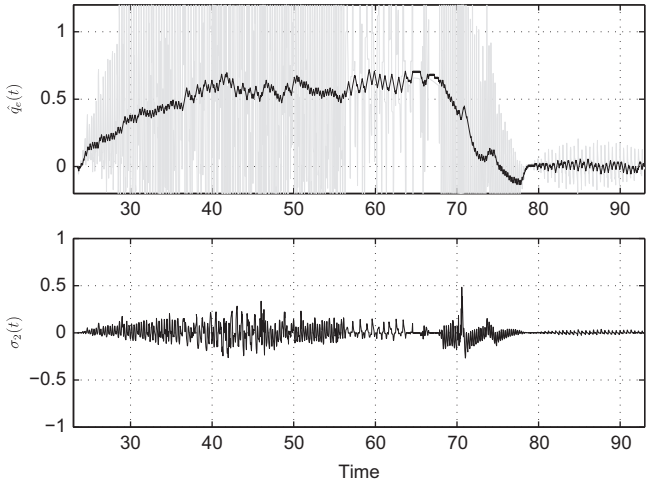

Fig. 4. Estimated specific ethanol production rate $\hat{q}_e(t)$ with SMO (black) and Eq. (29) (grey) (above); switching coordinate σ_2 (below).

Fig. 3 shows $\hat{\mu}(t)$ and the switching coordinate σ_1. In this fermentation the feeding profile was applied in open-loop operation, i.e. μ was not regulated by feedback. Recall that if steady-state operation of continuous fermentation is reached then $\mu=D$ (see Eq. (27a)). However, it can be seen between hours 67 and 79 that μ was greater than D due to depletion of ethanol. This illustrates monitoring capabilities of the proposal.

The on-line estimation of $q_e(t)$ gives the net production of ethanol, i.e. the balance between excreted ethanol due to fermentative growth on s and consumed ethanol due to oxidative growth on e. Fig. 4 shows $\hat{q}_e(t)$ and the switching coordinate σ_2. The decrease observed in q_e from $t\approx 67$ h is in accordance with the growth observed in Fig. 3.

Eq. (29) presents the crude estimation of $\alpha(t)$ obtained by model inversion from (3)

$$\hat{\alpha}(t)=\boldsymbol{G}_p^{-1}\boldsymbol{K}_p^{-1}\left(\frac{d\boldsymbol{z}}{dt}+D\boldsymbol{z}-\boldsymbol{F}_p+\boldsymbol{Q}_p\right). \tag{29}$$

Although this solution is simpler than most of the proposed algorithms, the result is strongly affected by measurement noise as shown in Figs. 3 and 4 in grey lines. A possible solution would

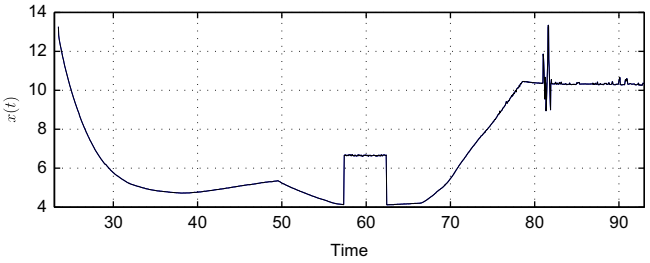

Fig. 5. Time profile of $x(t)$ with faults in measurement.

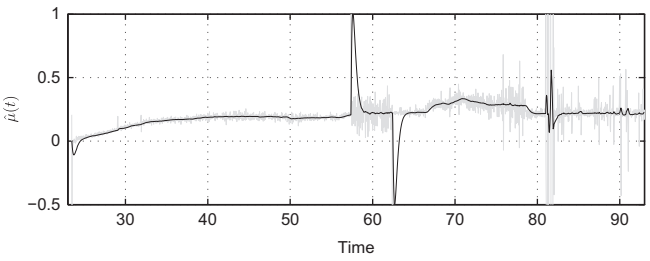

Fig. 6. Response under sensor failure with high gain observer: Eq. (26) vs Eq. (29).

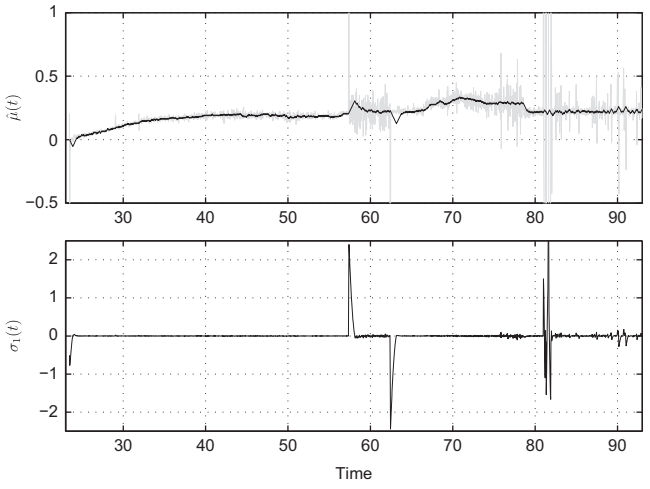

Fig. 7. Response under sensor failure for $\mu(t)$: SMO vs Eq. (29) (above) and switching coordinate (below).

be to add a lowpass filter, but the delay and filter dynamics could be detrimental in closed-loop configuration.

4.2. Comparison with high gain observers under sensor failure

Fig. 5 shows two typical sensor failures in biomass concentration measurement: a drift in the time interval [57,63] and some spikes at $t=81$ h. This type of problem should be early detected to take corrective actions. Note in Eqs. (27) that a problem in x affects estimation of both μ and q_e.

Algorithm (26) was initialised with the same conditions as the SMO. It was tuned with parameter $\theta_1 = 4.0$ looking for a comparable response with the SMO. Although θ_1 can be chosen high enough to ensure fast speed of convergence, this parameter tuning involves a trade-off between convergence speed and noise sensitivity. Besides, given its simplicity there is only one parameter to tune which in turn may be problematic when the measurements have different levels of noise (as in the case of biomass and ethanol measurements presented in Fig. 2).

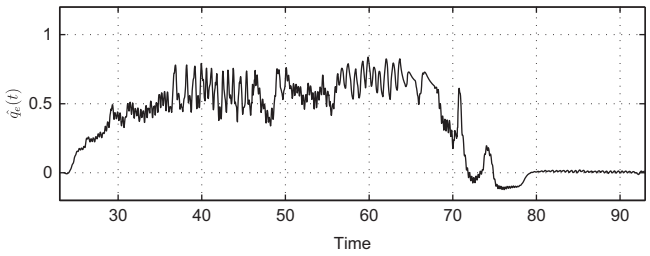

Fig. 8. Estimated specific ethanol production rate $\hat{q}_e(t)$ with high gain observer.

The result for the high gain algorithm under sensor failure is presented in Fig. 6. Given the drift in x, a response with large overshoot in $\hat{\mu}$ appears. Besides, the spikes in x generates additional fast changes in $\hat{\mu}$. Although this output behaviour shows a failure, it would not be acceptable in closed-loop control. On the other hand, the result of μ estimation with the SMO under the same scenario is presented in Fig. 7. As can be observed, the coordinate σ_1 early detects the fault exhibiting a problem detection feature of the proposal. Even more important, the effect of the drift on $\hat{\mu}$ is strongly reduced because the time derivative of each $\hat{\alpha}_i$ is bounded by the observer. In fact, the corresponding $\overline{\rho}_i$ allows to adjust that bound. Note that the spikes at $t=81$ h are completely rejected in the estimator and detected by the residual σ_1.

Finally, the result for q_e estimation is presented in Fig. 8. For the selected gain, the high gain approach exhibits worse response than the SMO until $t=70$ h.

5. Conclusions

The on-line kinetic rates estimation problem in bioprocesses was addressed. The proposed second-order SM observer is able to estimate multiple specific kinetic rates from related measurements of process variables even though no particular model of each kinetic rate was assumed.

Certainly, only upper bounds of the time derivatives are required. Global finite-time convergence is achieved by choosing a suitable observer structure. This property is particularly important in control applications because the observer does not add dynamics that might destabilise the closed loop.

The observer performance was assessed using experimental data from continuous-mode fermentation of *S. cerevisiae*. Microbial specific growth rate and net ethanol production rate were estimated. The proposed algorithm was compared with a high gain observer under normal operation and for two typical sensor faults. Particularly, the SMO showed better noise rejection in the noisiest signal and better transient response under sensor drifts and spikes.

Acknowledgements

This work was supported by ANPCyT (PICT-2011-0888), National University of La Plata (Project I164) and CONICET (PIP 112-2011-00361) of Argentina; and Universitat Politècnica de València (Grant FPI/2009-21) and FEDER-CICYT (DPI2011-28112-C04-01) of Spain and European Union.

References

Bastin, G., & Dochain, D. (1986). On-line estimation of microbial specific growth rates. *Automatica*, *22*, 705–709.

Bastin, G., & Dochain, D. (1990). *On-line estimation and adaptive control of bioreactors*. Elsevier.

Boyd, S., El Ghaoui, L., Feron, E., & Balakrishnan, V. (1994). Linear matrix inequalities in system and control theory. Studies in applied mathematics (Vol. 15). Society for Industrial and Applied Mathematics (SIAM).

De Battista, H., Picó, J., Garelli, F., & Navarro, J. L. (2012). Reaction rate reconstruction from biomass concentration measurement in bioreactors using modified second-order sliding mode algorithms. *Bioprocess and Biosystems Engineering*, *35*, 1615–1625.

De Battista, H., Picó, J., Garelli, F., & Vignoni, A. (2011). Specific growth rate estimation in (fed-)batch bioreactors using second-order sliding observers. *Journal of Process Control*, *21*, 1049–1055.

Edwards, C., & Spurgeon, S. (1998). *Sliding mode control: Theory and applications*. Taylor & Francis.

Evangelista, C., Puleston, P., Valenciaga, F., & Fridman, L. (2013). Lyapunov-designed super-twisting sliding mode control for wind energy conversion optimization. *IEEE Transactions on Industrial Electronics*, *60*, 538–545.

Farza, M., Busawon, K., & Hammouri, H. (1998). Simple nonlinear observers for on-line estimation of kinetic rates in bioreactors. *Automatica*, *34*, 301–318.

Gauthier, J., Hammouri, H., & Othman, S. (1992). A simple observer for nonlinear systems applications to bioreactors. *IEEE Transactions on Automatic Control*, *37*, 875–880.

Jobé, A. M., Herwig, C., Surzyn, M., Walker, B., Marison, I., & von Stockar, U. (2003). Generally applicable fed-batch culture concept based on the detection of metabolic state by on-line balancing. *Biotechnology and Bioengineering*, *82*, 627–639.

Karakuzu, C., Türker, M., & Öztürk, S. (2006). Modelling, on-line state estimation and fuzzy control of production scale fed-batch baker's yeast fermentation. *Control Engineering Practice*, *14*, 959–974.

Levant, A. (1998). Robust exact differentiation via sliding mode technique. *Automatica*, *34*, 379–384.

Löfberg, J. (2012). Automatic robust convex programming. *Optimization Methods and Software*, *27*, 115–129.

Martinez-Guerra, R., Garrido, R., & Osorio-Miron, A. (2001). Parametric and state estimation by means of high-gain nonlinear observers: Application to a bioreactor. In *Proceedings of the American control conference* (Vol. 5, pp. 3807–3808).

Moreno, J. A., & Osorio, M. (2008). A Lyapunov approach to second-order sliding mode controllers and observers. In *47th IEEE conference on decision and control, 2008. CDC 2008* (pp. 2856–2861).

Navarro, J., Pico, J., Bruno, J., Pico-Marco, E., & Valles, S. (2001). *On-line method and equipment for detecting, determining the evolution and quantifying a microbial biomass and other substances that absorb light along the spectrum during the development of biotechnological processes.* Patent ES20010001757, EP20020751179.

Perrier, M., Feyo de Azevedo, S., Ferreira, E., & Dochain, D. (2000). Tuning of observer-based estimators: *Theory and application to the on-line estimation of kinetic parameters*. *Control Engineering Practice*, *8*, 377–388.

Picó, J., De Battista, H., & Garelli, F. (2009). Smooth sliding-mode observers for specific growth rate and substrate from biomass measurement. *Journal of Process Control*, *19*, 1314–1323.

Rahman, A. F. N. A., Spurgeon, S. K., & Yan, X.-G. (2010). A sliding mode observer for estimating substrate consumption rate in a fermentation process. In *11th International workshop on variable structure systems*.

Ren, H., & Yuan, J. (2005). Model-based specific growth rate control for *Pichia pastoris* to improve recombinant protein production. *Journal of Chemical Technology and Biotechnology*, *80*, 1268–1272.

Shimizu, H., Takamatsu, T., Shioya, S., & Suga, K.-I. (1989). An algorithmic approach to constructing the on-line estimation system for the specific growth rate. *Biotechnology and Bioengineering*, *33*, 354–364.

Shtessel, Y., Moreno, J., Plestan, F., Fridman, L., & Poznyak, A. (2010). Super-twisting adaptive sliding mode control: A Lyapunov design. In *49th IEEE conference on decision and control (CDC)* (pp. 5109–5113).

Soons, Z., Voogt, J., van Straten, G., & van Boxtel, A. (2006). Constant specific growth rate in fed-batch cultivation of Bordetella pertussis using adaptive control. *Journal of Biotechnology*, *125*, 252–268.

Utkin, V., Guldner, J., & Shi, J. (1999). *Sliding mode control in electromechanical systems* (1st ed.). London: Taylor & Francis.

Venkateswarlu, C. (2004). Advances in monitoring and state estimation of bioreactors. *Journal of Scientific & Industrial Research*, *63*, 491–498.

Vojinovi, V., Cabral, J., & Fonseca, L. (2006). Real-time bioprocess monitoring. Part I: *In situ sensors*. *Sensors and Actuators B: Chemical*, *114*, 1083–1091.